

## Defect Content Evaluation in Single-Crystal AlN Wafers

Robert T. Bondokov<sup>1</sup>, Kenneth E. Morgan<sup>1</sup>, Raj Shetty<sup>1</sup>, Wayne Liu<sup>1</sup>, Glen A. Slack<sup>1</sup>, Mark Goorsky<sup>2</sup>, and Leo J. Schowalter<sup>1</sup>

1 - Crystal IS, Inc. 70 Cohoes Av., Green Island, NY 12183, USA

2 - Department of Materials Science and Engineering, UCLA, Los Angeles, CA 90095, USA

### ABSTRACT

Aluminum nitride (AlN) offers exceptional properties necessary to explore the development of large area substrates for nitride based electronics and photonics. Recent studies on AlN bulk growth using the sublimation-recondensation method developed at Crystal IS demonstrated high-quality crystals with low dislocation density and crystallographic uniformity. The diameter enlargement of these AlN boules is often associated with extensive defect generation. The goal of this study is to evaluate the origin and distribution of growth defects in AlN bulk crystals.

AlN crystals were grown using the sublimation-recondensation technique and then they were sliced into wafers. The defect evaluation in this study was performed using x-ray topography, differential image contrast and polarized-light optical microscopy, atomic force microscopy (AFM) and etch pit pattern delineation. Special attention was paid to crack development and propagation, grain boundary distribution, micro-scale inhomogeneities as well as to the origin and density of dislocations. The major cause of growth defect appears to be non-linearity of both axial and radial temperature gradients. Growth optimization results in lower defect density and improved crystallinity of the AlN crystals.

### INTRODUCTION

Nitride-based, III-V wide bandgap materials possess special interest for high-power and high-frequency electronics as well as for visible and ultraviolet (UV) photonics. The development of native nitride-based substrates with low defect density is required in order to produce high performance devices, while uniform, large area substrates are necessary for cost-effective device fabrication. Pure aluminum nitride offers exceptional properties such as high thermal conductivity, a large bandgap, natural insulating behavior, and high break-down voltage.

The bulk crystals of AlN were grown by the sublimation-recondensation method which was originally studied by Slack and McNelly [1] and further developed at Crystal IS [2]. These crystals demonstrate excellent x-ray crystallinity (typically  $< 30$  arcsec) and very low dislocation densities ( $\sim 10^3$  cm<sup>-2</sup>). Recently, Crystal IS has shown promising scalability of the growth method and crystal boules larger than 25mm in diameter were demonstrated. Increasing the wafer diameter and usable area are critical conditions for successful emergence of AlN as a nitride-based electronics substrate. Besides the above-mentioned advantages of AlN, it should be noted here that the crystal growth methods and temperatures utilized allow excellent polytype control producing only the stable 2H polytype (the 4H-AlN polytype was shown to appear when using 4H-SiC substrates as a seed [3]). In addition, we have demonstrated the ability to produce non-polar substrates which are being studied with increased interest.

The sublimation-recondensation method represents sublimation of a source material, vapor transport of Al and N<sub>2</sub> species driven by thermal gradients, and nucleation of crystalline AlN material. Clearly, producing large-area substrates increases the probability of defect generation due to naturally involved higher temperature gradients. There are certain types of defects in AlN that can be responsible for low quality Al<sub>x</sub>Ga<sub>1-x</sub>N epitaxial growth, high deep-UV optical absorption, and overall poor device performance. This study attempts to evaluate the AlN crystal growth-associated defects that may hinder further nitride-based electronics development. Our focus included defects such as cracks, grain boundaries, and dislocations: all of which affect wafer quality from the device application point of view. Special attention was paid to defect visualization and their classification.

## EXPERIMENTAL DETAILS

Bulk AlN single crystals were grown at Crystal IS using the sublimation-recondensation technique. The growth method, setup details and specific regimes were previously described elsewhere [4, 5]. AlN crystals were oriented and sliced into wafers and then carefully polished in order to obtain low roughness, sub-surface damage-free substrates. Surface finish was evaluated in terms of atomic force microscopy (AFM). The etch pit pattern delineation requires smooth, mirror-like surfaces before etching so that defect origin is well defined by the different etch pits. A triple-crystal x-ray diffractometer was used to establish x-ray topography images and to obtain the rocking curves. A typical rocking curve is present in Fig. 1 showing excellent crystallinity where the FWHM is about 10 arcsec.

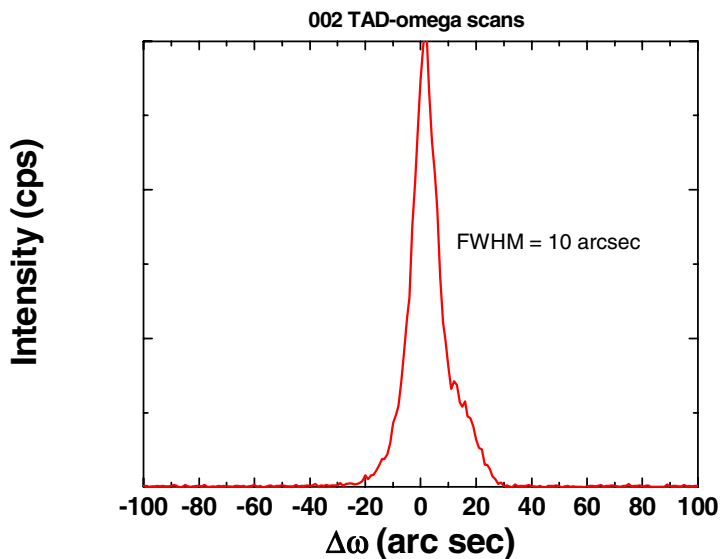


Fig. 1 A typical x-ray rocking curve from a 25 mm diameter AlN wafer.

Polarized light was used to make low resolution images where birefringence was used to evaluate the stress uniformity in wafers that have been oriented with the surface normal parallel to the *c*-axis (so-called on-axis wafers). These images were also used to distinguish between stress-induced non-uniformities and the presence of differently oriented grains. In some cases, we were able to observe cracking and related phenomena. In addition, we used Nomarski differential image contrast (NDIC) and chemical etching in order to reveal dislocation-related etch pits.

## RESULTS AND DISCUSSION

As a part of the micro-scale evaluation, we studied the birefringence to help identify the presence of cracks as well as their distribution and behavior. An AlN sample exhibiting cracks is shown in Fig. 2. Until recently it was thought that, as for the many crystals with the hexagonal closed packed (hcp) structure, aluminum nitride shows evidence of three basal plane glide systems  $\frac{1}{3}\langle 11\bar{2}0 \rangle\{0001\}$ . However, it is also known that in the case of  $\frac{c}{a} < 1.63$ , where *c* and *a* are the lattice constants, the prismatic glide system  $\frac{1}{3}\langle 11\bar{2}0 \rangle\{1\bar{1}00\}$  would be primary for such crystals. For AlN, this ratio is  $\frac{4.9816}{3.1127} = 1.600$  and hence the prismatic glide would be preferable. Prismatic glide was experimentally confirmed and observed for AlN ceramics between 500° and 800°C [6]. Evidence of this prismatic glide activation for AlN single crystal is shown in Fig. 3 where the straight lines represent slip bands oriented parallel to the  $\langle 1\bar{1}00 \rangle$  directions. These were revealed after chemical etching. Dots on Fig. 3 represent etch pits located at dislocation sites. It should be noted here that, unlike the 4H- and 6H-SiC crystals, AlN demonstrates cleavage cracking in most cases and shear cracks are almost negligible. Both SiC polytypes show basal plane glide and therefore prismatic slip is minimal [7] while shear stresses play a critical role in elastic-plastic relations at elevated temperatures. Another reason for the fact that prismatic glide is primary in hcp-crystals can be the presence of twins which can act as barriers to basal slip in hcp materials [8]. However, we have not observed any twins in AlN while using the most recent growth methods developed at Crystals IS.



Fig. 2 Cracking in AlN samples: a) optical image and b) corresponding birefringence image. Cracks are marked by the white arrows.

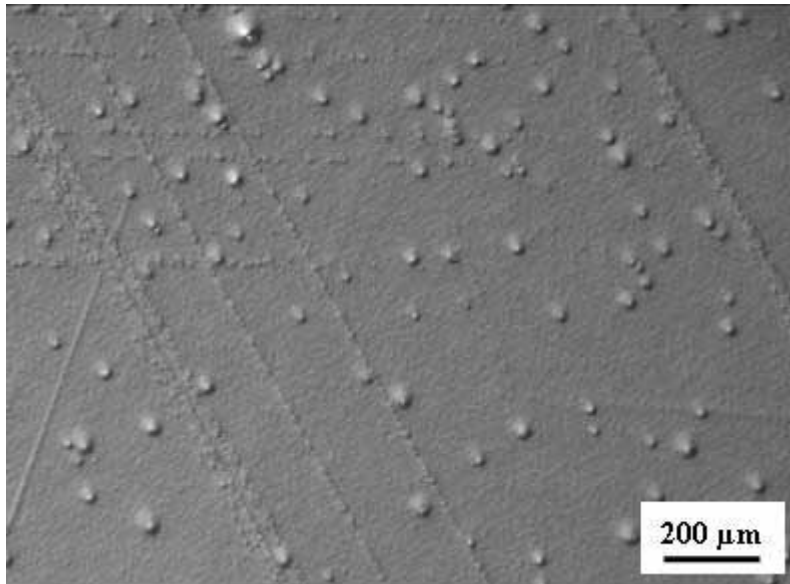


Fig. 3 NDIC image of prismatic slip bands as seen on on-axis oriented AlN after chemical etching

The presence of grains and grain boundaries in the AlN wafers was evaluated using birefringence contrast images. Fig. 4a represents the use of birefringence contrast images to highlight the distribution of grains. The AlN sample shown in Fig. 4 is on-axis oriented to within  $\pm 0.5^\circ$ . On a micro-scale grain boundaries can develop into slit defects, especially near crystal edges where the gradient curvature is higher. An example of slit defects at the AlN wafer edges is shown in Fig. 4b (dark field contrast image). In addition, we focused on sub-grain boundaries and their propagation as grain boundaries or even cracks. Fig. 4c demonstrates sub-grain boundaries (on the left) propagating as cracks into another grain (right). The sub-grain boundaries were revealed by chemical etching.

The evaluation of the dislocation content was carried out using a chemical etching technique. Details on the technique will be reported separately. We were able to reveal different types of etch pits and associate them with different defects. A typical etch pit pattern observed on the nitrogen-face of an AlN c-axis wafer is shown in Fig. 5.

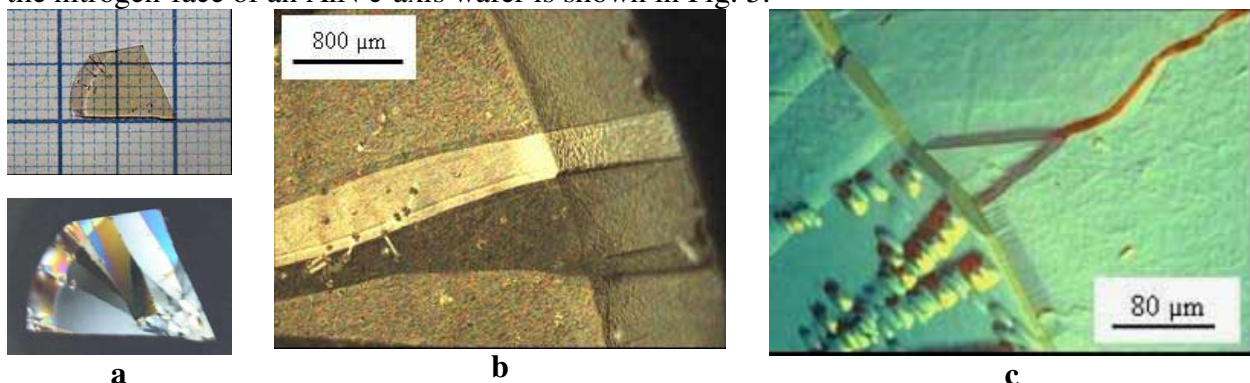


Fig. 4 Grains, grain boundaries and sub-grain boundaries in AlN wafers: a) low resolution optical image (top) and corresponding birefringence image, b) slit defects near a sample edge, c) NDIC image of sub-grain boundaries propagating into cracks.

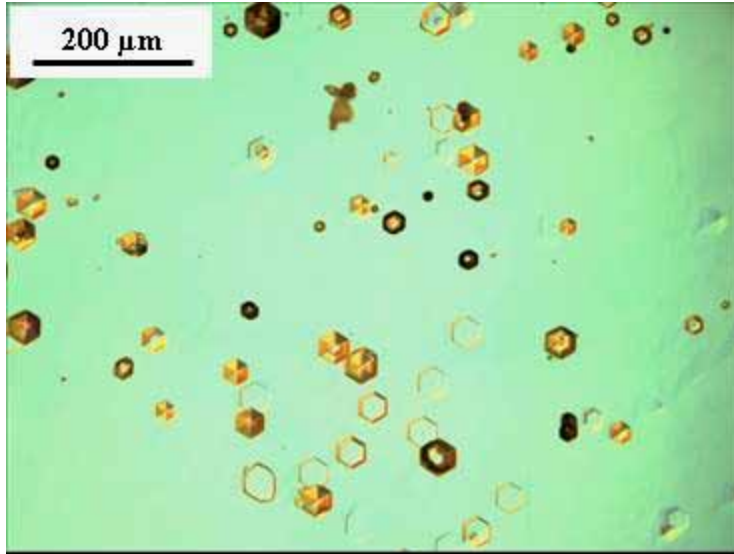
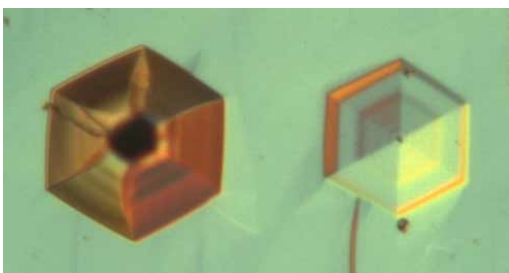


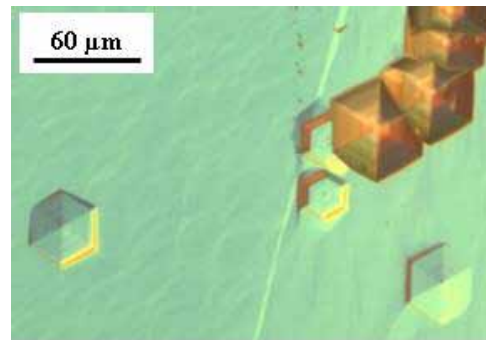
Fig. 5 NDIC image of dislocations in AlN revealed by chemical etching.

The average etch pit density (EPD) for c-oriented AlN wafers varies from  $1 \times 10^3$  to  $3 \times 10^4$   $\text{cm}^{-2}$ . The dislocation density is consistent with x-ray topography measurements [9]. Screw dislocations were identified by corresponding spiral step patterns on the surface when observed by AFM. Therefore, we associate one etch pit to one dislocation only. Our etch pit pattern technique allows us to simply distinguish between screw and pure edge types of dislocations. As seen from Fig. 6a, some of the screw dislocations exhibit an open core (left) while others have a closed core (right). The pure edge dislocations shown in Fig. 6b exhibit two different features: the closely-spaced darker ones (right top) correspond to edge dislocations that form grain boundaries walls while the other widely-spaced edge dislocations are usually due to the interactions with crucible walls and other defects.

For the first time, we present here the etch pits associated with the prismatic plane  $\{1\bar{1}00\}$  surfaces (Fig. 7). It is easy to see that etch pits follow the symmetry of the prismatic plane in AlN. The average etch pit density on the prismatic planes is from  $6 \times 10^4$  to  $4 \times 10^5$   $\text{cm}^{-2}$  and is shown since it is a clear example of the different kinds of etch pits seen although the density of observed dislocations is higher than typical.



a



b

Fig. 6 Etch pits associated with different types of dislocations: a) screw dislocations and b) edge dislocations.

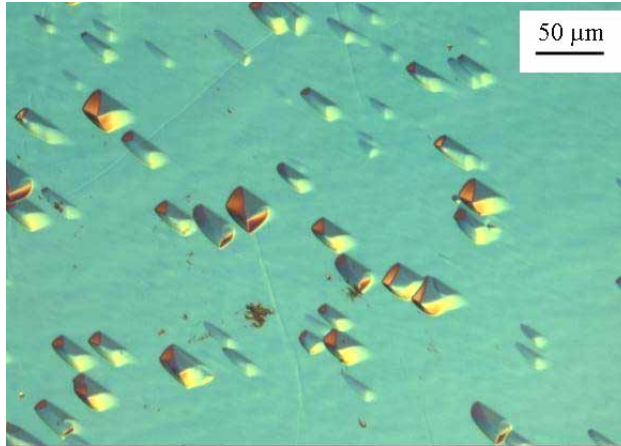


Fig. 7 Etch pits as revealed on the prismatic plane of AlN.

The observation that the prismatic plane dislocation density is two orders of magnitude higher on the basal plane surface suggests that there is simultaneous action of basal plane dislocations and a limited amount of dislocations generated as a result of stress removal during the cool-down process.

## CONCLUSIONS

High quality single crystal AlN boules were grown and characterized. A Majority of the defects that can affect the quality of the epitaxial AlGaIn nitride-based devices were evaluated. We found that the prismatic glide system can play an important role in the elastic-plastic transitions at elevated temperatures. In addition we report chemical etching results that help distinguish between etch pits caused by different types of dislocations. For the first time etch pits associated with dislocations penetrating the prismatic plane surfaces were revealed.

## ACKNOWLEDGEMENT

This work has been partially supported by NIST Advanced Technology Program, award number 70NANB4H3051.

## REFERENCES

1. G. A. Slack and T.F. McNelly, *J. Cryst. Growth* **34**, 263 (1976).
2. L. J. Schowalter, G. A. Slack, J. B. Whitlock, K. Morgan, S. B. Schujman, B. Raghathamachar, M. Dudley, and K. R. Evans, *phys. stat. sol. (c)* **0**, 1997 (2003).
3. N. Onojima, J. Suda, T. Kimoto, and H. Matsunami, *Appl. Phys. Lett.* **83**, 5208, (2003).
4. J.C. Rojo, G. A. Slack, K. Morgan, B. Raghathamachar, M. Dudley, L. J. Schowalter, *J. Cryst. Growth* **231**, 317 (2001).
5. J.C. Rojo, L.J. Schowalter, G. A. Slack, K. Morgan, J. Barani, S. Schujman, S. Biswas, B. Raghathamachar, M. Dudley, M. Shur, R. Gaska, N.M. Johnson, M. Kneissl, *Mat. Res. Soc. Symp. Proc.* **722**, K1.1.1, (2002).
6. V. Audurier; J.L. Demenet; J. Rabier, *Phil. Mag. A* **77**, 825, (1998).
7. M. Skowronski, *Materials Science Forum* **389-393**, 385, (2002).
8. A. Serra, D.J. Bacon, and R.C. Pond, *Metallurgical and Materials Trans. A* **33A**, 809 (2002).
9. B. Raghathamachar, M. Dudley, J.C. Rojo, K. Morgan, and L. J. Schowalter, *J. Cryst. Growth* **250**, 244 (2003)